RESEARCH PAPER

The bounding effect of the water retention curve on the cyclic response of an unsaturated soil

Arash Azizi[1,2] · Ashutosh Kumar[2,3] · David Geoffrey Toll[2]

Abstract

The water retention properties of soils present in formation layers of roads and railways continuously vary due to repeated traffic loads and periodic rainfall events. This is important because the accumulated deformation and resilient modulus of such soils under cyclic loading are profoundly affected by water retention properties. This paper discusses the cyclic and water retention response of a clayey sand subjected to repetitive cyclic loading and wetting stages. The results show that the accumulated permanent strains and resilient modulus of the tested soil are dependent on the suction level while the main wetting water retention curve of the soil dictates the variation of the suction measured during cyclic loading and wetting. This bounding effect of the water retention curve is found to be dependent on the void ratio where the suction can even increase due to the accumulation of strains under cyclic loading while the degree of saturation increases. This contradicts the suction reduction typically observed with an increase in the degree of saturation. A void ratio dependent water retention model is developed accounting for the observed bounding effect and employed to predict the measured suction during repetitive cyclic loading and wetting. The suction values predicted by the void ratio dependent water retention model are in good agreement with the experimental data. The predicted suctions are then used in semi-empirical formulations to obtain the accumulated permanent strains and resilient modulus. A better correlation between model predictions and experimental data is achieved where the suction values predicted by the void ratio dependent water retention model are used. The results imply that predictive frameworks proposed for the cyclic behaviour of road and railway formation layers require water retention counterparts that incorporate the bounding effect of void ratio on soil water retention curves.

Keywords Cyclic loading · Suction · Unsaturated soil · Water retention curve

1 Introduction

A precise description of soil water retention behaviour is crucial to understand the performance of compacted soils used for construction of transportation infrastructure. This is because changes in water retention properties, i.e. suction and water saturation level, of such soils due to seasonal variations can significantly alter the response of formation layers of roads and railways subject to cyclic traffic loads and hence affect serviceability of road pavements and railway tracks (e.g. [15, 20, 24, 33, 35]). Experimental results of cyclic testing showed that the response of unsaturated soils is dependent on soil water retention properties while information on both suction and water saturation levels are required to evaluate the accumulated permanent deformation and resilient modulus (e.g.

✉ Arash Azizi
   arash.azizi@port.ac.uk

   Ashutosh Kumar
   ashutosh@iitmandi.ac.in

   David Geoffrey Toll
   d.g.toll@durham.ac.uk

[1] School of Environment, Geography and Geosciences, University of Portsmouth, Portsmouth, UK

[2] Department of Engineering, Durham University, Durham, UK

[3] School of Engineering, IIT Mandi, Mandi, India

[7, 14, 21, 28, 46]). Therefore, any interpretive framework developed for the cyclic response of unsaturated soils requires a water retention counterpart that recognises the evolution of soil suction and water saturation under cyclic loading conditions (e.g. [2, 7, 34]).

The relationship of soil water retention properties has been found to be hysteretic between drying (evaporation) and wetting (precipitation) [13], implying that the suction level of a formation soil at a certain water content is not unique. This hysteretic soil water retention behaviour is described by transitional scanning paths bounded by main drying and wetting water retention curves (e.g. [10, 30, 40, 42]). The bounding effect of the water retention curve is dependent also on soil density or void ratio (e.g. [1, 11, 25]). Gallipoli et al. [11] demonstrated that a decrease in the void ratio can shift soil water retention curves to higher saturation levels and vice versa. This has been reported to dictate the water retention behaviour and hence the volumetric and shear response of unsaturated soils to monotonic loading, for example in the case of a compacted clay tested under the direct shear condition [37] and a compacted silt sheared under the triaxial compression condition [26]. However, the bounding effect of soil water retention behaviour under cyclic loading has not previously been addressed mainly due to difficulties associated with the measurement of soil water retention properties during cyclic testing [16, 27].

Kumar et al. [18, 19] showed that accurate measurements of degree of saturation and suction during cyclic triaxial testing can be achieved using an on-specimen monitoring system including miniature displacement transducers and a suction probe mounted at the mid-height (close to the shear zone) of unsaturated soil specimens. The results showed that the soil water retention response to cyclic loading was governed predominantly by the distance between the current soil water retention state and the main water retention curves while the changes in the void ratio also affected the water retention behaviour under cyclic loading. However, the bounding effect of the water retention behaviour and its contribution to accurate predictions of accumulated permanent strains and resilient modulus of the tested soil subjected to cyclic loading has not previously been considered.

In this study, the cyclic and water retention response of a compacted clayey sand to repetitive loading cycles and staged wetting (following the testing approach described in Kumar et al. [18]) are examined and the bounding effect of the water retention curve on the variations of soil suction during repetitive cyclic loading and wetting stages are discussed. A water retention model is developed to predict the water retention behaviour of the tested soil and suction variations measured during repetitive loading cycles and staged wetting in which the suction values are predicted by incorporating the effect of the void ratio. The predicted suction values are then used in semi-empirical formulations to predict the accumulated permanent strains and resilient modulus measured for the tested soil.

2 Testing methodology

The tested soil was a clayey sand (79% sand, 12% silt and 9% clay) taken from the fill material below the sub-ballast layer of a railway embankment constructed along the south-eastern coast of South Africa. The clay fraction of the tested soil is Hymod Prima [12], plastic Ball Clay consisting of disordered kaolinite, micaceous material, and quartz. The same soil has commonly been used in research studies, see for example Gräbe & Clayton [12], Mamou et al. [23] and Blackmore et al. [7]. The specimens were compacted in a compaction mould with a height of 200 mm and a diameter of 100 mm using a drop hammer following the standard Proctor test procedure [5]. Specimens of 70 mm in diameter and 140 mm in height were then trimmed and recovered from the compaction mould. The compaction condition of the specimens was similar to the field compaction condition, i.e. an average density of 1.84 Mg/m^3 and water content of 10.8%, i.e. just wet of the optimum w_{opt} = 10.2%.

They were then air-dried to a water content of about 7% while being exposed to a constant room temperature of 20 °C ($\pm$ 0.5 °C) and relative humidity of 34%. At the end of drying, the specimens were wrapped and sealed in a plastic bag for more than 24 h for water equalisation. The specimens were then mounted on the triaxial pedestal while the suction of the specimens was monitored using a suction probe under a constant water content condition. Water equilibrium was assumed to be achieved when the probe measured a constant suction value.

The suction probe used is a high capacity tensiometer capable of measuring positive and negative water pressures in a range of 2 MPa with a resolution of $\pm$ 0.5 kPa [22, 38]. Properties of the tested soil and specimens prepared for tests of cyclic loading and staged wetting are presented in Table 1.

After applying a confining pressure σ_c of 20 kPa to the specimens assembled on the triaxial apparatus, they were repetitively subjected to cyclic loading and wetting including: (i) *cyclic loading stages*: 1000 cycles of a deviatoric stress q_{cyc} of 40 kPa (SWU40) and 80 kPa (SWU80) were applied at a frequency of 1 Hz while a resting deviatoric stress of 10 kPa and a constant confining pressure σ_c of 20 kPa were maintained as shown in Fig. 1a. The resting deviatoric stress was maintained to ensure continuous contact between the loading ram and the soil specimens during cyclic loading (ii) *wetting stages*: After

Table 1 Properties of the tested soil and prepared specimens

Tested soil	Sand % 79	Silt % 12	Clay % 9	Plasticity index 9	Specific gravity 2.66
Properties after drying	Density ρ_d (Mg/m³)	Water content w (%)	Suction s (kPa)	Degree of saturation S_r (%)	Void ratio e (–)
SWU40	1.841	7.29	259	43.57	0.444
SWU80	1.840	6.82	220	40.70	0.445
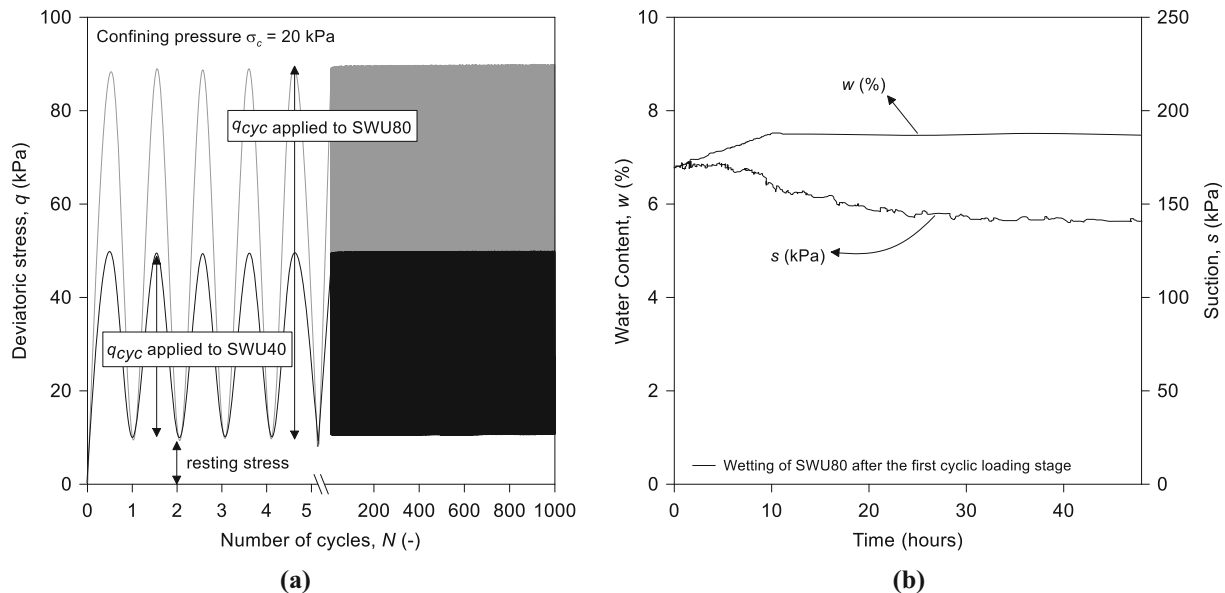
Fig. 1 Stages of repetitive cyclic loading and wetting **a** load cycles applied during cyclic loading stages **b** an example of water content and suction monitoring during the wetting stage

each cyclic loading stage (a packet of 1000 cycles), a certain amount of water was injected into the specimens from the top drainage line at a very small infiltration rate of about 1 g/h. The water content was obtained from back calculation based on the water content of the specimen measured at the end of the test and the amount of water injected at each wetting stage. Figure 1b shows an example of the increase in the water content and the monitored suction value of SWU80 during wetting imposed after the first cyclic loading stage.

During testing, the air pressure was at the atmospheric pressure while the negative pore water pressure, and hence suction, was continuously monitored using a suction probe mounted at the mid-height of the specimen. The cyclic loads were applied after a constant value of suction was measured at the end of the wetting stages ensuring a water equilibrium was achieved. The pattern of cyclic loading and wetting stages applied to the soil specimens are representative of a field condition of formation materials of roads and railways repetitively subjected to passing traffic and precipitation events. Details of the testing methodology

are explained in Kumar et al. [18]. Table 2 shows the description of the tests carried out.

3 Soil response to repetitive cyclic loading and wetting

Figure 2a shows that the axial strain ε_a of SWU80 continuously increased with the cyclic loading stages following the successive increases in the water content of the specimen due to wetting. In the case of SWU40 where the applied q_{cyc} was lower, the increase in ε_a was evident mainly during the first two loading stages while the strains measured after the second loading stage were very small although the soil water content repetitively increased during wetting stages.

Figure 2b shows the void ratio of the two specimens subsequently decreased due to the compressive volumetric strains measured during cyclic loading stages while the volumetric strains, and hence changes in void ratio, were negligible during the wetting stages (the maximum

Table 2 Description of the tests carried out

Test stage*	SWU40					SWU80				
	ρ_d (Mg/m^3)	w (%)	s (kPa)	S_r (%)	e (–)	ρ_d (Mg/m^3)	w (%)	s (kPa)	S_r (%)	e (–)
Compression	1.870	7.29	217	45.88	0.422	1.860	6.82	200	42.17	0.430
First loading	1.878	7.29	206	46.52	0.417	1.871	6.82	172	42.97	0.422
First wetting	1.877	9.11	84	58.14	0.417	1.871	7.53	146	47.48	0.422
Second loading	1.880	9.11	79	58.43	0.415	1.873	7.53	144	47.68	0.420
Second wetting	1.880	9.40	56	60.25	0.415	1.875	8.26	88	52.45	0.419
Third loading	1.881	9.40	53	60.31	0.414	1.881	8.26	92	53.09	0.414
Third wetting	1.881	10.79	24	69.28	0.414	1.881	8.95	62	57.48	0.414
Fourth loading	1.882	10.79	24	69.36	0.414	1.886	8.95	67	57.95	0.411
Fourth wetting	1.882	13.19	14	84.83	0.413	1.887	10.55	35	68.45	0.410
Fifth loading	1.883	13.19	15	84.97	0.413	1.893	10.55	40	69.21	0.406
Fifth wetting	–	–	–	–	–	1.912	12.83	28	87.28	0.391
Sixth loading	–	–	–	–	–	1.919	12.83	26	88.45	0.386

*The values measured at the end of each stage are reported

swelling volumetric strain measured during wetting was −0.08%). Similar to the trend of ε_a measured, the decrease in the void ratio of SWU80 was more evident than that of SWU40.

Figure 2c shows the increase in the degree of saturation S_r of SWU40 and SWU80 during the wetting stages due to the increase in their water content and also during the loading stages as the specimens exhibited compressive volumetric strains while their water content remained constant under cyclic loading.

During the wetting stages, the suction measured for SWU40 and SWU80 decreased associated with the increase in S_r as shown in Fig. 2d. Under cyclic loading, the suction measured for SWU40 continuously decreased during the first, second and third loading stages and remained almost constant during the last two loading stages as the changes in the measured volumetric strains (and hence the increase in S_r) were very small. The suction measured for SWU80 also decreased with the increases in S_r during the application of the first two and the last packets of cyclic loads but increased during the third, fourth and fifth cyclic loading stages (Fig. 2d) regardless of the measured increases in the degree of saturation. The reason for such behaviour, i.e. unexpected increases in the suction with increases in the degree of saturation, is explained later in the paper.

Figure 3a shows the accumulated permanent strain ε_p and suction s measured for the two specimens at the end of each cyclic loading stage. ε_p of SWU40 and SWU80 increased with the application of cyclic loads as the suction level successively and evidently decreased during the wetting stages. The diminishment of inter-granular bonding

due to reduction in suction facilitated the slippage of soil particles and led to accumulation of larger strains under cyclic loading. The measured ε_p also depended on the applied cyclic loads where the rate of the increase in ε_p of SWU80 having a higher q_{cyc} increased more evidently than that of SWU40 where the measured ε_p showed just a gentle increase after the second loading stage.

Figure 3b shows the resilient modulus M_R of the two specimens progressively decreased with the decrease in the suction levels since the stabilising effect of suction bonding reduced as the testing stages progressed. M_R measured for SWU40 was greater than that of SWU80 implying that applying a higher q_{cyc} reduced the soil resiliency as also observed by Yang et al. [43] and Ng et al. [27].

The measured accumulated permanent strains and resilient modulus show that the cyclic response of the tested soil was predominantly governed by the measured suction level and applied cyclic deviatoric stress. It should be noted that a complete resilient state was not achieved for these cases, but the differences were very small and would not lead to erroneous interpretation of the results.

The suction and degree of saturation of the two specimens measured at the end of cyclic loading and wetting stages are shown in Fig. 4. The main drying and wetting water retention curves of the tested soil are also redrawn from Kumar et al. [18]. The water retention states of these specimens were close to the main drying curve at the beginning of the tests as the specimens were air-dried to water content levels lower than those the specimens possessed after preparation. The subsequent increases in the degree of saturation during cyclic loading and wetting stages shifted their water retention state towards the main
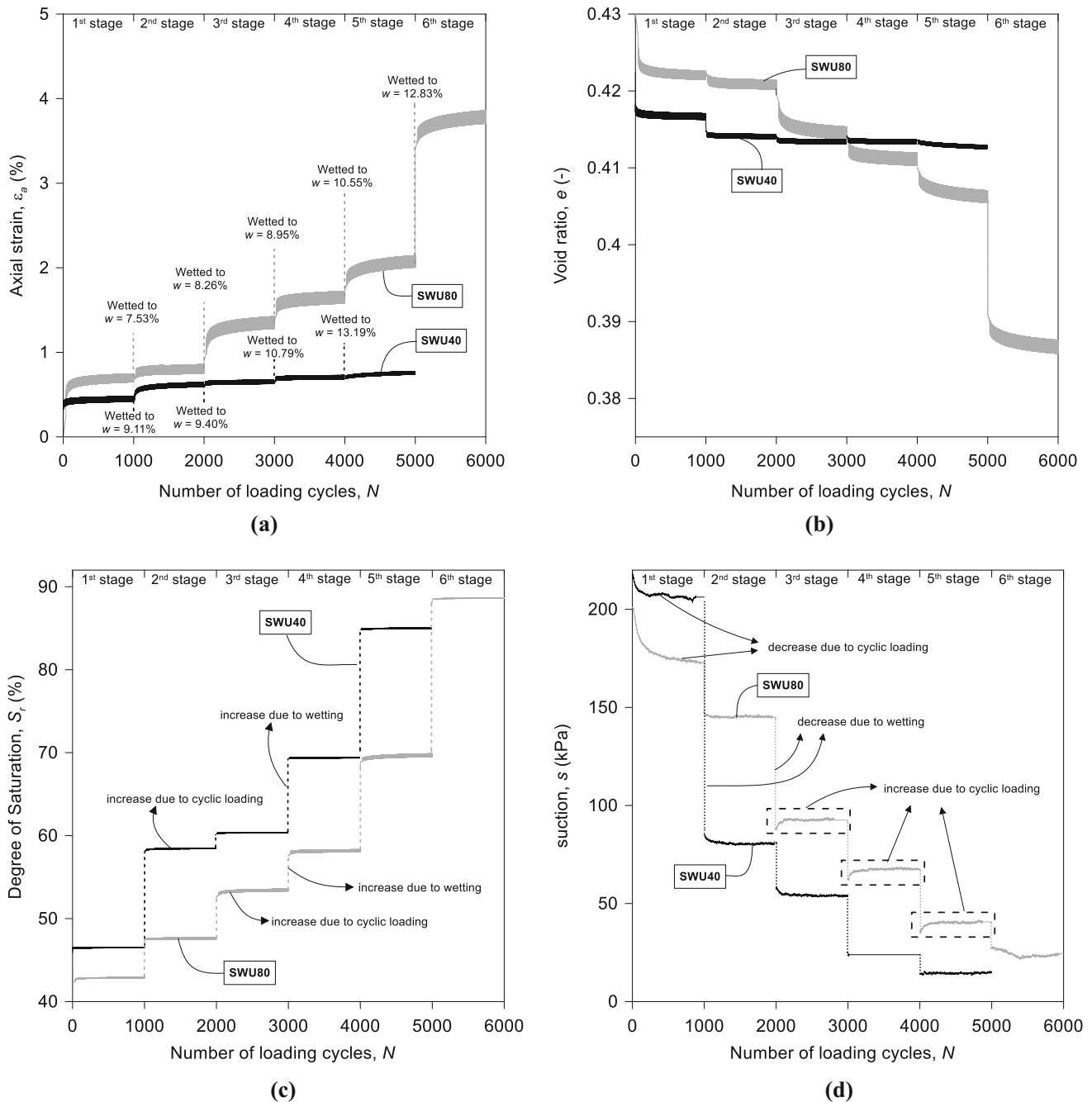
Fig. 2 Response of SWU40 and SWU80 to repetitive cyclic loading and wetting: **a** axial strain, ε_a **b** void ratio, e **c** degree of saturation, S_r **d** suction, s

wetting curve as the testing stages progressed. However, the suction values measured for SWU40 and SWU80 were greater than the corresponding suction value on the main wetting curve at a given saturation level. This was more evident in the case of SWU80 where the suction increased during the third, fourth and fifth cyclic loading stages as shown in Fig. 4. This can be explained by introducing the effect of the changes in the void ratio measured during testing on the soil water retention curve.

4 Bounding effect of water retention curve

Figure 5 shows the water retention paths traced by SWU40 and SWU80 where the labels of the data points are the void ratio measured at the end of cyclic loading stages. The water retention contours for the wetting path of the tested soil are also shown to discuss the void ratio dependent nature of the water retention behaviour of these two specimens. It is worth mentioning that all these curves are
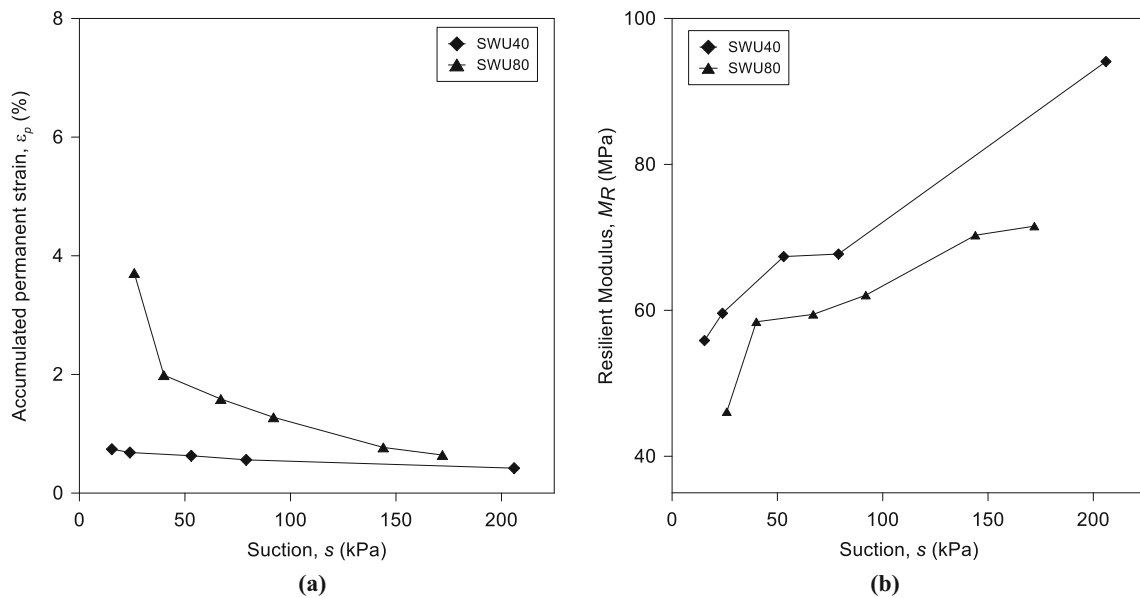
Fig. 3 **a** accumulated permanent strains ε_p with suction **b** resilient modulus M_R with suction
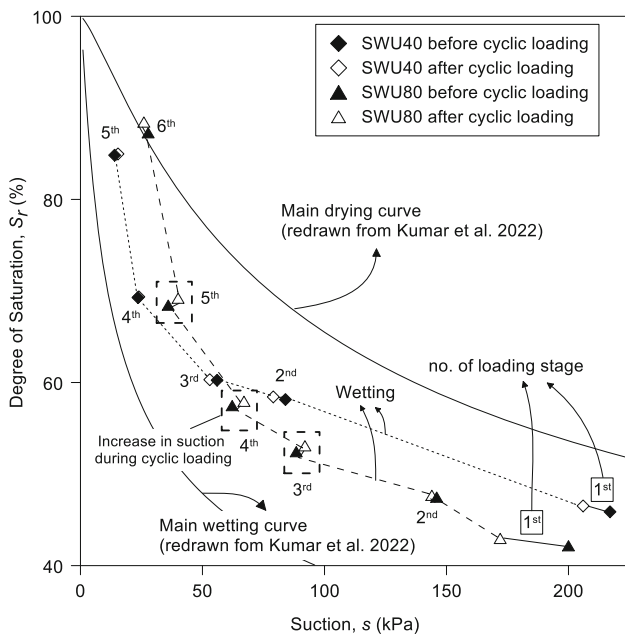

Fig. 4 Water retention behaviour of SWU40 and SWU80 during repetitive cyclic loading and staged wetting

predicted by the void ratio dependent model developed and described later in this paper.

Figure 5a shows the water retention state of SWU40 during repetitive cyclic loading and wetting while the main wetting water retention curve of the tested soil at the void ratio of $e_o = 0.434$ is assumed based on the experimental data reported by Kumar et al. [18]. The initial void ratio of SWU40 was 0.422 while it reduced to 0.415 during the first two loading stages and remained almost constant during the following loading stages as shown in Fig. 5a. The

initial decrease in the void ratio affected soil water retention behaviour where the water retention path traced by the specimen as well as the main wetting water retention curve obtained for the tested soil at $e_0 = 0.434$ shifted to higher suction levels.

Figure 5a also shows that a shifted main wetting water retention curve corresponding to $e = 0.415$ for the tested specimen can be detected while the water retention state of SWU40 followed this shifted curve. After the second loading stage, the suction changes of SWU40 during cyclic loading and wetting were bounded by the shifted curve while no further shift of the main wetting water retention curve took place as the void ratio of SWU40 remained almost constant.

In the case of SWU80, the void ratio continuously decreased from 0.430 to 0.386 as the loading stages progressed, leading to subsequent shifts of the water retention path traced by the specimen as shown in Fig. 5b. With the accumulation of strains, several shifted main wetting water retention curves are incorporated accounting for the effect of the successive decreases in the void ratio of SWU80. The suction of SWU80 reduced during the first two loading and wetting stages while the suction level was greater than that of the shifted curve assumed for $e = 0.422$ at a given degree of saturation, implying that the water retention state of the soil lies within the scanning domain above the main wetting curve. For the following loading and wetting stages, the changes in the suction were bounded as the water retention state of SWU80 met the shifted main wetting water retention curve corresponding to $e = 0.414$. After the second loading stage, the suction of SWU80 reduced during wetting following the shifted curves due to
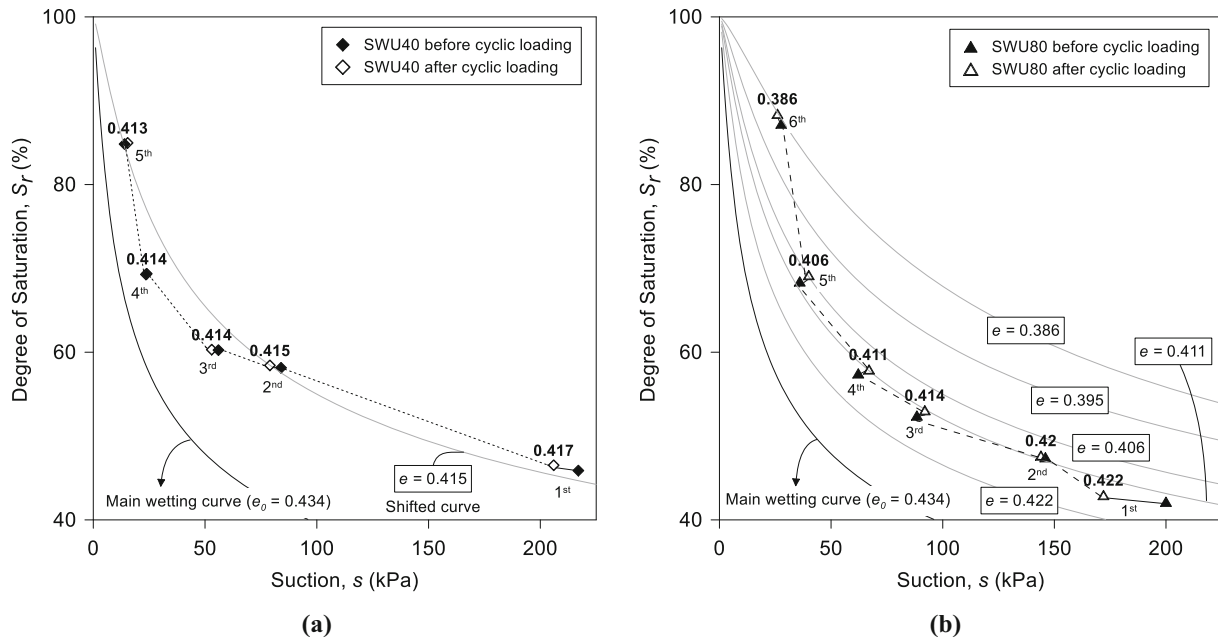
Fig. 5 Effect of void ratio on water retention behaviour: **a** SWU40 **b** SWU80

the increase in the degree of saturation. However, the suction increased during the loading stages as the main wetting water retention curve continued to shift to the higher suction levels with the further decreases in the void ratio due to the applied cyclic loads (e.g. the water retention curve shifted with the decrease in void ratio from 0.412 to 0.406 during the fifth cyclic loading stage where the suction of SWU80 increased from 35 to 40 kPa as shown in Fig. 5b). This implied that the water retention behaviour of SWU80 was also bounded by the main wetting water retention curve in which the reduction in the void ratio and the shift of the water retention curve resulted in the increase in the suction of SWU80 although the degree of saturation increased during cyclic loading.

The results show that the water retention behaviour of the soil subjected to repetitive cyclic loading and staged wetting is bounded by the main wetting water retention curve while changes in the void ratio due to the successive accumulation of strains dictate the suction variations of the tested soil during cyclic loading and wetting. The suction measured is found to increase even when the degree of saturation increases as the decrease in the void ratio shifted the bounding water retention curve to higher suction levels. A similar bounding effect of main water retention curves on soil behaviour under monotonic loading was observed and discussed by Tarantino & Tombalato [37] and Musso et al. [26] where the shift of the main drying water retention curve resulted in the decrease in the soil suction while the degree of saturation reduced.

5 Developing the soil water retention model

The experimental results indicated the bounding effect of the water retention curve on the cyclic behaviour of the tested soil. In the following, an attempt was made to show that a water retention model that incorporates the effect of mechanical parameters such as void ratio can properly predict the water retention behaviour of the tested soil under cyclic loading while a water retention model that neglects such an effect is not able to capture the bounding effect of the soil water retention curve discussed earlier in this paper.

A water retention model was developed to predict the water retention behaviour of the tested soil while distinct formulations were used for predicting scanning and main water retention curves. The model for the wetting path is discussed here as $\Delta S_r > 0$ was always the case during cyclic loading and wetting stages. The proposed water retention model includes:

(i) a formulation proposed by van Genuchten [41] to predict the main wetting water retention curve where $S_r = S_{rw}$ (S_{rw} is the degree of saturation on the main wetting curve):

$$S_{rw} = \frac{1}{\left(1 + \alpha_w s_w{}^{n_w}\right)^{1 - \frac{1}{n_w}}} \tag{1}$$

where α_w and n_w are model parameters. It can be observed from the formulation that the effect of void ratio on soil water retention curve is not incorporated in the original model (called "void ratio independent VG model" in this

paper) as the degree of saturation is only dependent on suction.

α_w is related to the air occlusion value of the main wetting curve and can be defined to be dependent on void ratio (e) rather than a constant value (similar approaches were used by e.g. [11, 36]). Hence, considering the dependency of void ratio on the air occlusion value, a new model named "void ratio dependent VG model" was proposed where $\alpha_w = \beta(\frac{e}{e_0})^\psi$:

$$S_{rw} = \frac{1}{\left(1 + \beta(\frac{e}{e_0})^\psi s_w{}^{n_w}\right)^{1-\frac{1}{n_w}}} \qquad (2)$$

where e_0 is a reference (initial) void ratio, β and ψ are model parameters.

Developing a general soil water retention model that incorporates mechanical effects requires considering a detailed description of soil volumetric behaviour and the evolution of soil pore size distribution (see e.g. [3, 4, 8, 32, 44]). However, a simple approach was adopted here as the main aim was addressing the bounding effect of the water retention curve of the tested soil under cyclic loading. The empirical ratio of the current and initial void ratio ($\frac{e}{e_0}$) was found to efficiently incorporate the void ratio dependency of the water retention behaviour of the tested soil in which the predicted air occlusion value of the wetting water retention curve increases with the decrease in void ratio and vice versa.

(ii) an incremental formulation to predict the water retention curve in the scanning domain, i.e. above the main wetting curve where $S_r > S_{rw}$:

$$\Delta S_r = -k\left(\frac{s_w}{s}\right)\frac{\Delta s}{s} \qquad (3)$$

where k controls the shape of the scanning curve and s_w is the suction value on the main wetting curve at a given saturation level. The way this incremental formulation was developed is explained later in the paper.

Equation (3) relates the degree of saturation predicted within the scanning domain to the suction value on the main wetting curve (s_w) implying that this projected suction value at the current degree of saturation needs to be back calculated from the formulation proposed for the main water retention curve that is Eq. (1) in the case of the void ratio independent VG model or Eq. (2) in the case of the void ratio dependent VG model. Therefore, s_w used in Eq. (3) in the case of the void ratio independent VG model was obtained from Eq. (1) for a given S_r:

$$s_w = \left(\frac{(S_r)^{\frac{n_w}{1-n_w}} - 1}{\alpha_w}\right)^{\frac{1}{n_w}} \qquad (4)$$

where s_w only changes with degree of saturation.

In the case of the void ratio dependent VG model, s_w obtained by Eq. (2) was used in Eq. (3):

$$s_w = \left(\frac{(S_r)^{\frac{n_w}{1-n_w}} - 1}{\beta(\frac{e}{e_0})^\psi}\right)^{\frac{1}{n_w}} \qquad (5)$$

which allowed incorporating the effect of void ratio on the predicted scanning curves where s_w changes with both degree of saturation and void ratio.

In the following, the predictions of the water retention response of the tested soil to cyclic loading are compared considering the response predicted by (i) the void ratio independent VG model using Eq. (1) for the main wetting curve ($S_r = S_{rw}$) and eqs. (3) and (4) for the scanning curve ($S_r > S_{rw}$), and (ii) the void ratio dependent VG model using Eq. (2) for the main wetting curve ($S_r = S_{rw}$) and eqs. (3) and (5) for the scanning curve ($S_r > S_{rw}$).

It has to be pointed out that the void ratio dependent water retention model was proposed as an example model to show that the bounding effect of the water retention curve on the cyclic behaviour of the tested soil (in this case a clayey sand) can be predicted. The simple phenomenological parameters used in the proposed water retention model can be calibrated using conventional water retention test results. The generalisation of the proposed formulations requires their validation using a wider range of experimental data and considering the behaviour of various soil types, particularly in the case of fine-grained soils with higher clay percentages where physiochemical characteristics of clay minerals and aggregate structures govern soil hydro-mechanical behaviour, which is not the scope of this paper (see details in e.g. [17, 31, 39, 45]).

6 Calibration of soil water retention model

The soil water retention models were calibrated using the scanning and main wetting water retention data of the tested soil (for the specimen compacted at a very similar state, $e_0 = 0.434$) reported by Kumar et al. [18] as shown in Fig. 6a. The water retention data showed that the data points obtained by the discrete measurements lay on the main wetting curve while the data obtained by the continuous measurements followed a scanning wetting path that met the main wetting curve at a suction of about 10 kPa.

Figure 6b shows the void ratio measured for the tested soil where the void ratio increased with the decrease in suction during continuous and discrete wetting tests. Equation (3) was used to predict the continuous wetting water retention curve (scanning curve) as it lies above the main wetting curve ($S_r > S_{rw}$) while eqs. (1) and (2) were used to simulate the discrete wetting water retention data
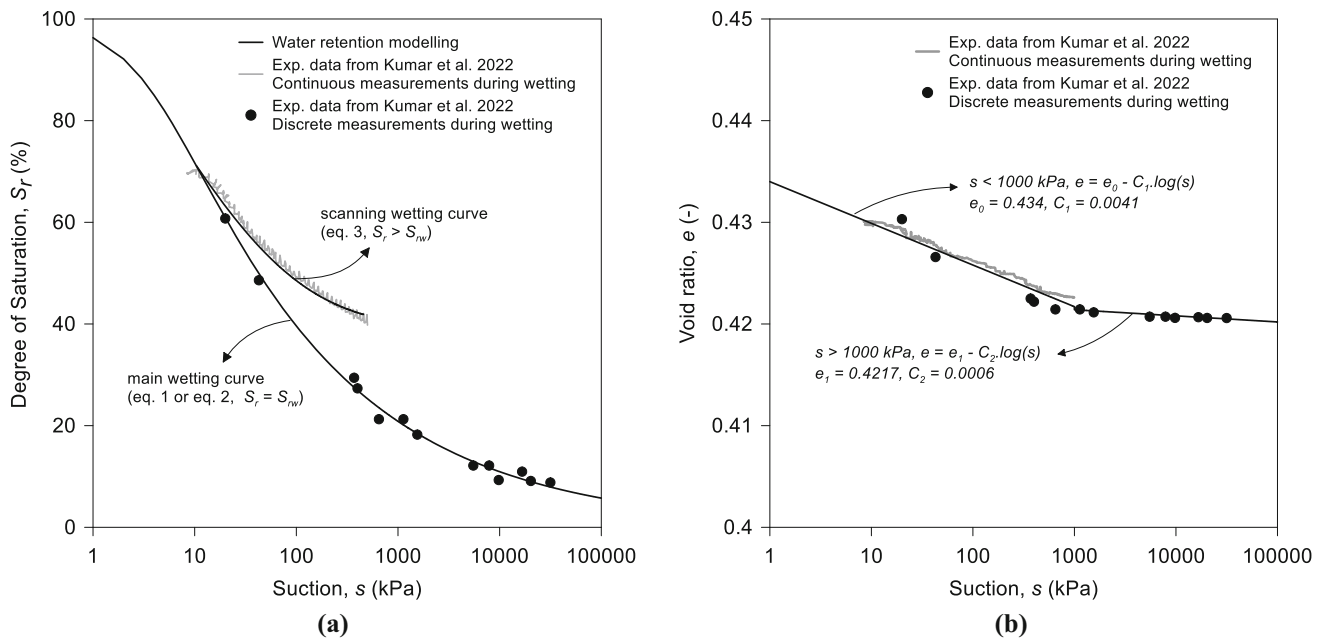
Fig. 6 Modelling water retention behaviour of the tested soil **a** the scanning and main wetting water retention curves **b** continuous and discrete measurements of void ratio during wetting

Table 3 Parameters of the water retention model used for the tested soil

Model	Parameters			
Void ratio independent VG	α_w		n_w	k
	0.270		1.280	0.140
Void ratio dependent VG	β	ψ	n_w	k
	0.262	17.925	1.310	0.120

associated with the main wetting curve ($S_r = S_{rw}$). In the case of the void ratio dependent VG model, the void ratio (e) used in Eq. (2) was predicted by two formulations associated with suction levels greater and smaller than 1000 kPa as shown in Fig. 6b. The initial void ratio $e_{o} = 0.434$ associated with the main wetting curve was assumed. Table 3 provides values of the parameters used.

Figure 6a also shows the model predictions of scanning and main water retention curves which are in good agreement with the experimental data while very similar water retention curves are predicted by the void ratio dependent and independent VG models. Equation (3) proposed to simulate scanning curves is based on a simple incremental formula: $\Delta S_r = -k\frac{\Delta s}{s}$ which is the derivative of a linear relationship $S_r = S_{r0} - k\log(s)$ where S_{r0} is the reference degree of saturation at $s = 1$ kPa. It was found that $-k\frac{\Delta s}{s}$ cannot closely predict the shape of the continuous experimental water retention data shown in Fig. 6a (represented in Fig. 7 where suction is shown in the natural scale).
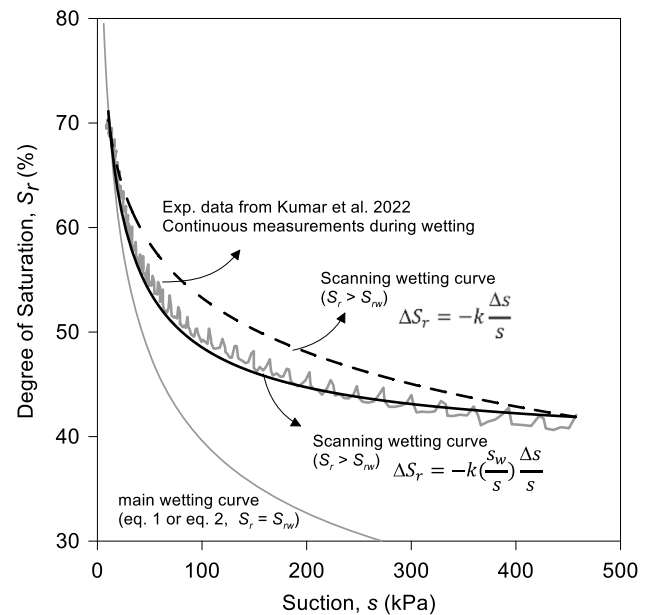

Fig. 7 Predictions of the continuous experimental data (scanning curves) using incremental formulations

Therefore, an additional term, i.e. $\frac{s_w}{s}$, was introduced into Eq. (3) to improve the predictions as it allows (i) predicting the continuous experimental water retention data very well (Fig. 7) and (ii) scanning curves to automatically shift with any changes in the main wetting water retention curve, for instance due to changes in the void ratio in the case of the void ratio dependent VG model.

For proper simulation of the scanning curve, $k = 0.14$ was adopted when Eq. (3) accompanied Eq. (1) (in the case of the void ratio independent VG model) whereas $k = 0.12$ was used when s_w obtained from Eq. (2) was used in Eq. (3) (in the case of the void ratio dependent VG model). As shown in Fig. 7, the scanning curves predicted by the void ratio independent and dependent VG models almost overlap since very similar s_w was predicted in both cases using different sets of parameters given in Table 3. It has to be noted that β and ψ were calibrated in a way to also capture the water retention behaviour of SWU40 and SWU80 as explained later in the paper.

7 Predicting soil water retention response to cyclic loading

The proposed water retention models were first used to predict the water retention response of the tested soil to cyclic loading using the experimental data taken from - Kumar et al. [18]. Figure 8a, b shows the suction and void ratio values of two specimens measured before and after cyclic loading while the cyclic deviatoric stress q_{cyc} was 40 kPa and the confining pressure σ_c was 20 kPa. The degree of saturation increased due to the compressive volumetric response (the decrease in the void ratio) of the soil under cyclic loading at the constant water condition. The degree of saturation (and the void ratio in the case of the void ratio dependent VG model) were used to predict

the changes in the suction measured during cyclic loading using the same parameters given in Table 3.

For both specimens ("T2" shown in Fig. 8a and "T5" shown in Fig. 8b), the suction was greater than the suction on the main wetting curve at a given degree of saturation $s > s_w$. Therefore, Eq. (3) for the scanning curve was rearranged to obtain suction variations $\Delta s = -\frac{s}{k}\left(\frac{s}{s_w}\right)\Delta S_r$ where s_w was obtained by Eq. (4) in the case of the void ratio independent VG model and by Eq. (5) in the case of the void ratio dependent VG model. The void ratio independent VG model overestimated the suction changes of T2 and T5 while the predictions of the void ratio dependent VG model were more consistent with the measured values.

The predicted s_w changes only with S_r in the case of the void ratio independent VG model (Eq. (4)) as the main wetting curve remains unchanged during cyclic loading (shown as the main wetting curve at $e_0 = 0.434$) while it is affected by S_r and e in the case of the void ratio dependent VG model (Eq. (5)). The decrease in the void ratio of T2 and T5 under cyclic loading shifts the main wetting curve (shown as the main wetting curves at $e = 0.439$ and $e = 0.425$ for T2 and at $e = 0.407$ and $e = 0.401$ for T5) resulting in the increase in s_w predicted by the void ratio dependent VG model and hence smaller suction variations predicted by $\Delta s = -\frac{s}{k}\left(\frac{s}{s_w}\right)\Delta S_r$ compared to those predicted by the void ratio independent VG model.

Figure 9 shows the predicted and measured suction variations of all specimens subjected to cyclic loading with respect to their suction values obtained before applying the cycles. The results show that the predictions of the void
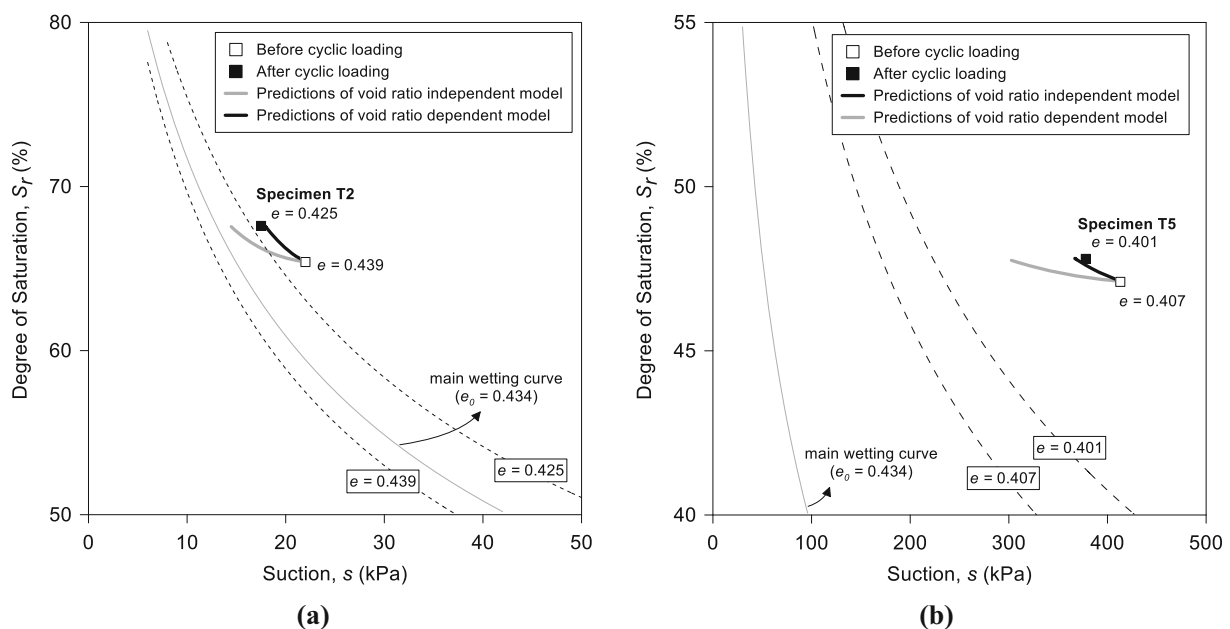

Fig. 8 Predictions of the suction measured before and after cyclic loading: a the water retention response of T2 b the water retention response of T5
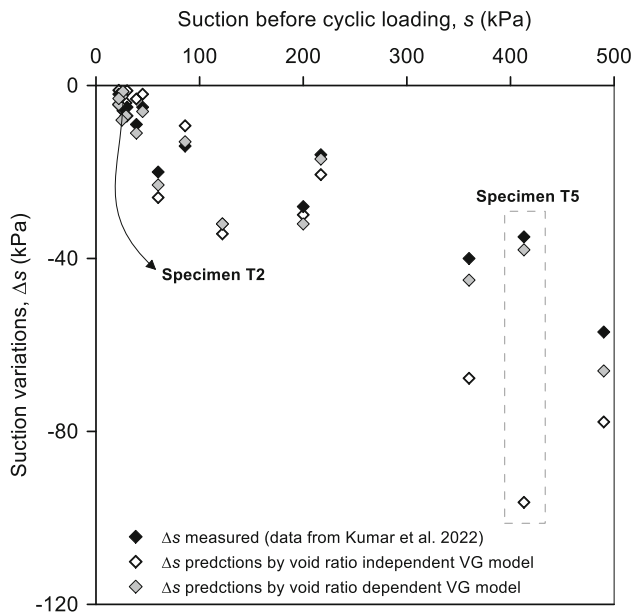
Fig. 9 Predictions of the water retention behaviour of the specimens subjected to cyclic loading

ratio dependent VG model are more accurate than the predictions of the void ratio independent VG model, particularly at suction levels greater than 200 kPa (e.g. where T5 is indicated) where the predicted and measured suction values are in good agreement when the void ratio effect is incorporated.

8 Predicting soil water retention response to repetitive cyclic loading and staged wetting

The proposed water retention models were eventually used to predict the suction measured during repetitive cyclic loading and staged wetting and address the bounding effect of the water retention curve discussed earlier in this paper.

The measured values of the degree of saturation (and the void ratio in the case of the void ratio dependent VG model) were used to predict the evolution of suction. For the scanning domain where $s > s_w$, $\Delta s = -\frac{s}{k}\left(\frac{s}{s_w}\right)\Delta S_r$ was used where s_w was obtained by Eq. (4) in the case of the void ratio independent VG model and by Eq. (5) in the case of the void ratio dependent VG model. For the main wetting domain where $s = s_w$, the suction was directly predicted by Eq. (1) or Eq. (2).

Figure 10 shows the measured and predicted water retention behaviour for SWU40 subjected to repetitive cyclic loading and staged wetting. The suction values predicted by the void ratio independent VG model are shown in Fig. 10a where the predicted s_w is also plotted. The void ratio independent VG model predicted suction

reductions with the increase in S_r during the first testing stages using Eq. (3) as $s > s_w$ while s_w (Eq. (4)) changed with the increase in S_r and followed the main wetting curve of the tested soil corresponding to $e_o = 0.434$ as shown in Fig. 10a. For the last two loading stages (fourth and fifth), Eq. (1) was used as the water retention state of SWU40 met the main wetting curve ($s = s_w$).

Figure 10b shows the predicted suction values where the effect of void ratio was incorporated using the void ratio dependent VG model. In this case, s_w predicted by Eq. (5) changed with the void ratio as well as the degree of saturation. s_w increased with the decrease in the void ratio of SWU40 and the main wetting curve shifted to higher suction levels during the first two loading stages as shown in Fig. 10b. After the second cyclic loading stage, the shifted water retention curve remained almost constant as the void ratio of SWU40 showed no significant changes during the following cyclic loading stages. Hence, Eq. (3) used for the void ratio dependent VG model predicted lower suction variations and higher suction values during initial testing stages due to the increase in s_w until the water retention state of SWU40 met the shifted main wetting curve at a suction of 40 kPa. During the following loading and wetting stages, the suction reduces with the increase in S_r following the shifted wetting curve predicted by Eq. (2) proposed for the main wetting curve. Figure 10b shows that the void ratio dependent VG model predicted smaller decreases in suction where better predictions of the water retention behaviour of SWU40 during repetitive cyclic loading and staged wetting were obtained.

Figure 11a shows the predicted and measured suction values for SWU80 where the void ratio independent VG model predicted suction reductions with the successive increases in the degree of saturation as the testing stages progressed. The void ratio independent VG model evidently underestimated suction values as the predicted s_w changed only with S_r and the water retention state of SWU80 following the main water retention curve corresponding to $e_o = 0.434$. The predicted scanning curve just met the main wetting at a low suction level about 20 kPa (the 5th cyclic loading stage) as shown in Fig. 11a. The predicted suction reductions were also in disagreement with the suction increments measured during the third, fourth and fifth cyclic loading.

As shown in Fig. 11b, the suction values predicted by the void ratio dependent VG model were greater than those predicted by void ratio independent VG model as Eq. (3) predicted lower suction reductions due to the increase in s_w associated with the decrease in the void ratio during cyclic loading (predicted by Eq. (5)). The water retention state of SWU80 followed the shifted main wetting water retention curve after the third loading stage where $s = s_w$. In the following stages, the suction values predicted by Eq. (2)
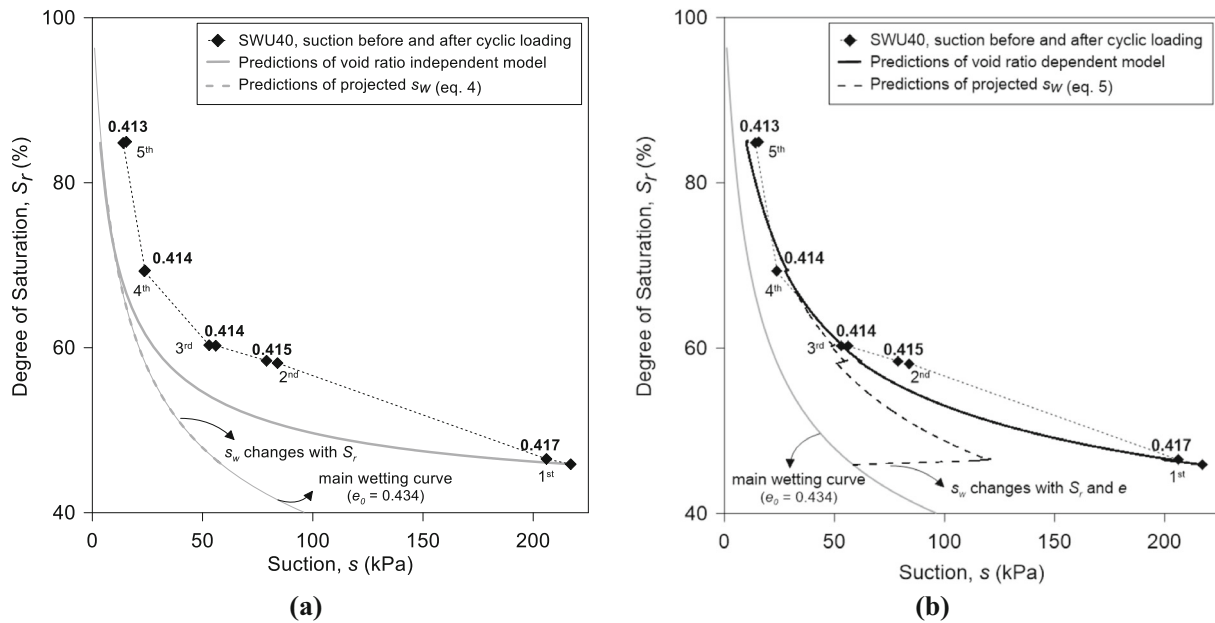
Fig. 10 Experimental data and model predictions of water retention behaviour of SWU40: **a** void ratio independent VG model **b** void ratio dependent VG model
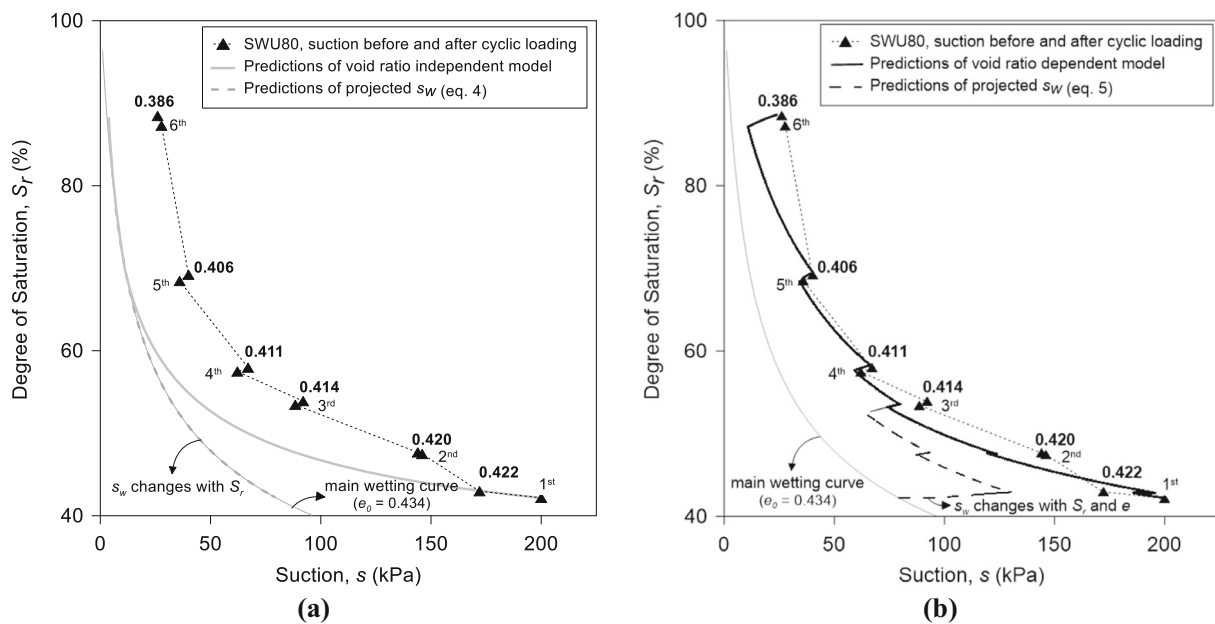

Fig. 11 Experimental data and model predictions of water retention behaviour of SWU80: **a** void ratio independent VG model **b** void ratio dependent VG model

proposed for the main wetting curve reduced during the wetting stages as the void ratio changes were very small and the water retention behaviour was dominantly governed by the increase in S_r. However, the void ratio of SWU80 continuously decreased during cyclic loading stages leading the main water retention curve to subsequently shift to higher suction levels as predicted by the void ratio dependent VG model (Fig. 11b). The

experimental data and model predictions for SWU80 were in a good agreement where the effect of the void ratio on the water retention behaviour was incorporated.

Figure 12 compares the suction values measured at the end of cyclic loading stages and those predicted by the void ratio dependent and independent VG models. The accuracy of the predicted suction levels for SWU40 (Fig. 12a) and SWU80 (Fig. 12b) is evidently improved where the effect
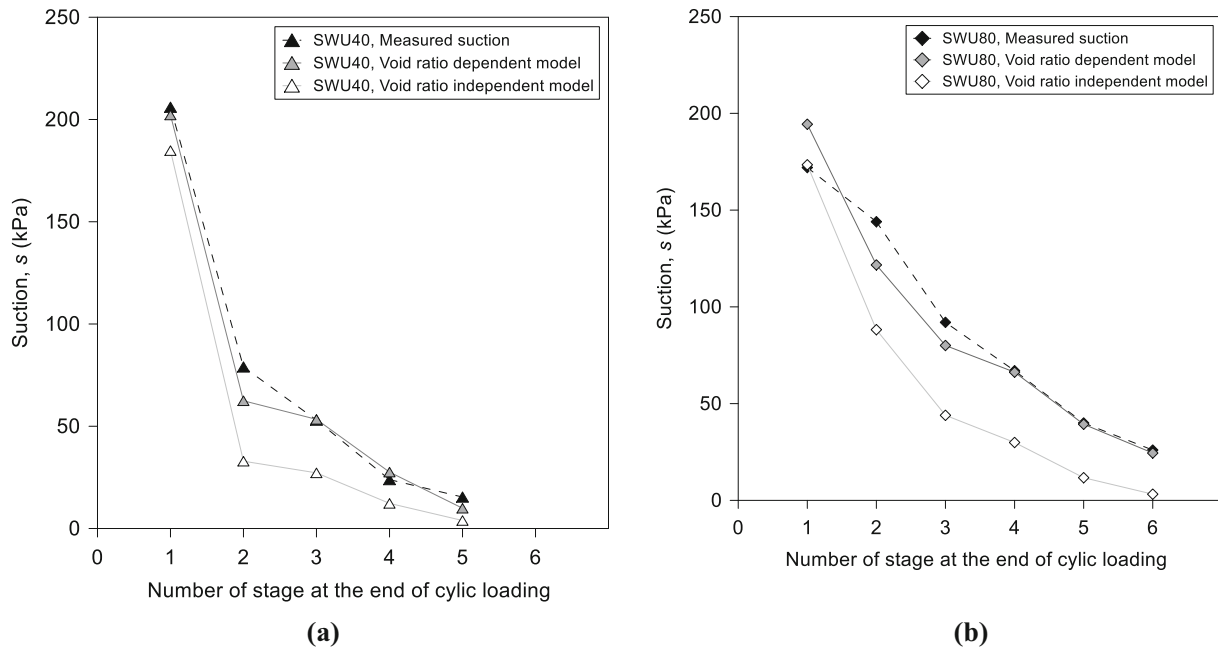
Fig. 12 Measured and Predicted values of suction at the end of cyclic loading stages **a** SWU40 **b** SWU80

of the void ratio is incorporated. The results showed that accounting for the bounding effect of the void ratio on of the water retention curve allows capturing the water retention behaviour of the tested soil subjected to repetitive cyclic loading and wetting well and also predicting unexpected increases in the suction with increases in the degree of saturation.

9 Predicting soil cyclic response incorporating suction

In this section, the importance of accurate predictions of suction for modelling soil cyclic response are discussed. The main aim is showing that using a void ratio dependent model to predict the water retention response of the tested soil to cyclic loading can improve predictions of accumulated permanent strains and resilient modulus using an existing model that relies on suction for modelling the cyclic behaviour of unsaturated soils. Several predictive models have been proposed for the cyclic response of unsaturated soils incorporating water retention properties such as volumetric water content (e.g. [28]), degree of saturation (e.g. [7]) and suction (e.g. [27]). Azizi et al. [2] proposed a framework to predict the accumulated permanent strain and resilient modulus accounting for the effect of suction using two constitutive variables: Bishop's stress accounting for soil skeleton stress and a bonding parameter accounting for the inter-granular force due to the presence of water menisci within soil pores. Semi-empirical

formulations proposed by Azizi et al. [2] were used in this study to predict the soil response to repetitive cyclic loading and staged wetting where suction values predicted by the void ratio dependent and independent VG models were incorporated. The model required the calculation of mean Bishop's stress ratio η^*:

$$\eta^* = \frac{q_{cyc} + q_r}{p^*} \tag{6}$$

where q_{cyc} and q_r are cyclic and resting deviatoric stresses and p^* is mean Bishop's stress [6], $p^* = p_n + S_r s$, p_n is mean net stress (the difference between the total stress and air pressure). The bonding parameter ξ [11] was obtained from:

$$\xi = (1 - S_r)f_s \tag{7}$$

where f_s accounts for the increase in the inter-granular force with suction and is estimated by $f_s = 0.838s^{0.06}$ that adequately fit the values suggested by Fisher [9] assuming a soil consists of identical spherical particles having radii of 1 μm. The accumulated permanent strain was predicted then by:

Table 4 Parameters of the models used to predict the cyclic behaviour of the tested soil

Model parameters for predicting ε_p	n_1	n_2	m_1	m_2	α
	19.7	7.3	91.2	5.2	0.3
Model parameters for predicting M_r	k_1	k_2	k_3	M_0	
	2.57	2.52	0.73	46	

$$\varepsilon_p = \eta^{*f_\xi} \left[f'_\xi (1 + m_1 f'^{(m_2-1)}_\xi \eta^{*(\alpha-f_\xi)}) \right] \tag{8}$$

where

$$f_\xi = n_1 \exp(-n_2\xi) \tag{9}$$

and

$$f'_\xi = \frac{1}{1 + \exp(\xi)} \tag{10}$$

n_1, n_2, m_1, m_2 and α are model parameters.

The formulation used to predict the resilient modulus M_R was as follows:

$$M_R = (p^*/p_r)^{k_1} \cdot (1 + q_{cyc}/p_r)^{-k_2} + M_0\exp(k_3\xi) \tag{11}$$

where $p_r = 1$ is the reference mean stress (in kPa). k_1, k_2, M_0 and k_3 are model parameters. The parameters reported by Azizi et al. [2] for the cyclic behaviour of the same soil tested in the present study were used in the numerical calculation (Table 4).

Figure 13a shows model predictions and experimental data of the accumulated permanent strains ε_p and suction values for SWU40 and SWU80 subjected to repetitive cyclic loading and staged wetting. The model predicted the increase in the accumulated permanent strains with the decrease in suction. This is because the soil tendency to deform increased as Bishop's stress and the suction bonding parameter decreased with the reduction of suction. ε_p obtained by using the suction values predicted by the void ratio independent VG model significantly overestimated the measured values for SWU40 at all suction levels and for SWU80 at low suction levels. As discussed earlier, the suction values predicted by the void ratio dependent VG model were greater and closer to the measured experimental data than those predicted by the void ratio independent VG model, leading to higher values of Bishop's stress and the bonding parameter. This implies that the soil was assumed to be more stable while its volumetric deformations under cyclic loading were constrained in the case where the suction was predicted by the void ratio dependent VG model. Therefore, Eq. (8) predicted lower ε_p and values closer to the experimental data of SWU40 and SWU80.

Figure 13b shows that the predicted resilient modulus M_R for SWU40 and SWU80 decreased with the successive cyclic loading stages as Bishop's stress and suction bonding decreased with the suction reductions. M_R obtained for SWU40 incorporating the suction values predicted by the void ratio independent VG model was underestimated. The predicted Bishop's stress and the bonding parameter increased where greater suction values predicted by the void ratio dependent VG model were incorporated which led to predictions of greater M_R values and closer to the

experimental data. This trend was also observed in the case of SWU80 where the void ratio dependent VG model predicted the resilient modulus more accurately than the void ratio independent model as shown in Fig. 13b.

It is to be noted that the accuracy of the predictions of the cyclic behaviour of the tested soil discussed earlier is not exclusively dependent on the predicted suction levels but also on the predictive capability of the formulations used to obtain the accumulated permanent strains and resilient modulus. Although the formulations used were not only dependent on suction, the predictions generally improved where more accurate suction values predicted by the void ratio dependent VG model were incorporated. The effect of accurate predictions of suction is expected to be even more pronounced in the models proposed for soil cyclic behaviour where the unsaturated state of the soil is only introduced in terms of suction (e.g. models proposed by [14, 27]).

10 Conclusions

Repeated traffic loads and periodic precipitations continuously alter water saturation and suction levels of compacted soils used in formation layers of roads and railways. In the present study, the cyclic and water retention response of a compacted clayey sand to repetitive cyclic loading and staged wetting is first discussed. Next, a water retention modelling framework is developed accounting for the effect of the hysteretic and void ratio dependent nature of water retention curves. The developed water retention model was then used to predict the suction variations of the soil specimens under repetitive cyclic loading and wetting. The predicted suctions were also employed in semi-empirical formulations to predict the cyclic response of the tested soil.

The experimental results showed a successive accumulation of permanent strains whereas the resilient modulus subsequently reduced as the testing stages progressed. A progressive loss of suction during wetting and also with the application of cyclic loads was observed where the soil specimen was subjected to the cyclic deviatoric stress of 40 kPa. In the case of the cyclic deviatoric stress of 80 kPa, the suction decreased during wetting but increased during a few cyclic loading stages although the degree of saturation continuously increased. This increase in the suction was explained by the bounding effect of the void ratio dependent soil water retention curve. The accumulation of volumetric strains and the subsequent decreases in the void ratio, which was more evident in the case of the cyclic deviatoric stress of 80 kPa, shifted the water retention state of the tested soil towards higher suction levels at a given degree of saturation.
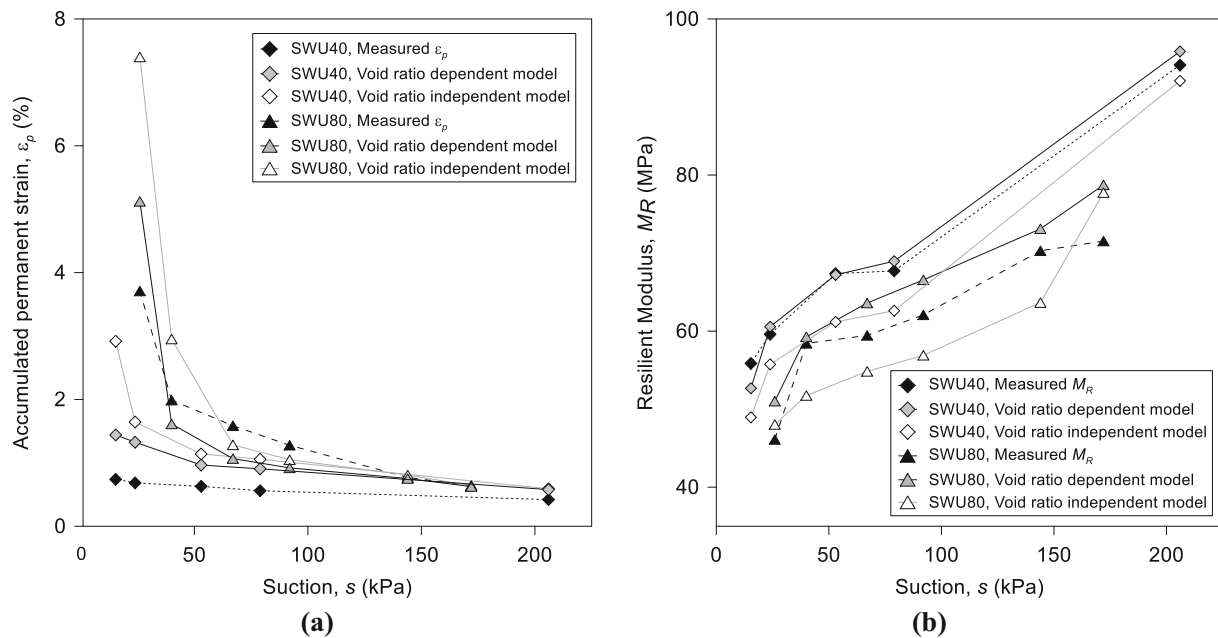
Fig. 13 Experimental data and model predictions of cyclic response of SWU40 and SWU80 in terms of the measured suction **a** accumulated permanent strain ε_p **b** resilient modulus M_R

A hysteretic water retention model was then developed based on the water retention data of the tested soil along drying and wetting path while the effect of the void ratio was also incorporated. The void ratio dependent water retention model was then employed to predict the water retention response of the soil specimens to repetitive cyclic loading and wetting. These predictions were compared to those where the effect of the void ratio was neglected. A good agreement between the soil water retention behaviour and model predictions during repetitive cyclic loading and wetting was obtained where the effect of void ratio was considered. The void ratio dependent water retention model allowed accounting for the bounding effect of the water retention curve and predicting the shift in the water retention curves and suction increments although the degree of saturation increases.

The predicted suctions were then used in semi-empirical formulations to predict the accumulated permanent strains and resilient modulus measured for the tested soil during repetitive cyclic loading and wetting stages. The experimental data were predicted more accurately where suction values obtained by the void ratio dependent water retention model were used. This implies that predictive frameworks proposed for the cyclic behaviour of formation layers of transportation infrastructure require water retention counterparts that can accurately predict the changes in water retention properties of the unsaturated soil subjected to coupled traffic and environmental loading. Such predictions can be obtained by considering the bounding effect of

the water retention curve and incorporating the effect of void ratio on soil water retention behaviour.

References

1. Azizi A, Jommi C, Musso G (2017) A water retention model accounting for the hysteresis induced by hydraulic and mechanical wetting-drying cycles. Comput Geotech 87:86–98
2. Azizi A, Kumar A, Toll DG (2021) Coupling cyclic and water retention response of a clayey sand subjected to traffic and environmental cycles. Géotechnique. https://doi.org/10.1680/jgeot.21.00063

3. Azizi A, Musso G, Jommi C (2020) Effects of repeated hydraulic loads on microstructure and hydraulic behaviour of a compacted clayey silt. Can Geotech J 57(1):100–114

4. Azizi A, Kumar A, Lingwanda MI, Toll DG (2020) The influence of rates of drying and wetting on measurements of soil water retention curves. In: Volume 195 of Proceedings, 4th European conference on unsaturated unsaturated soils, E3S Web of Conference, 03005. Lisboa, Portugal: EDP Sciences

5. BSI (British Standards Institution) (1990) Method of test for soils for civil engineering purposes: compaction related test. BS 1377-4. London: BSI

6. Bishop AW (1959) The principle of effective stress. Tecknisk Ukeblad 106(39):859–863

7. Blackmore L, Clayton CRI, Powrie W, Priest JA, Otter L (2020) Saturation and its effect on the resilient modulus of a pavement formation material. Géotechnique 70(4):292–302

8. Casini F, Vaunat J, Romero E, Desideri A (2012) Consequences on water retention properties of double-porosity features in a compacted silt. Acta Geotech 7(2):139–150

9. Fisher RA (1926) On the capillary forces in an ideal soil: correction of formulae given by WB Haines. J Agric Sci 16(3):492–505

10. Gallipoli D, Bruno AW, D'Onza F, Mancuso C (2015) A bounding surface hysteretic water retention model for deformable soils. Géotechnique 65(10):793–804

11. Gallipoli D, Wheeler SJ, Karstunen M (2003) Modelling the variation of degree of saturation in a deformable unsaturated soil. Géotechnique 53(1):105–112

12. Gräbe PJ, Clayton CR (2009) Effects of principal stress rotation on permanent deformation in rail track foundations. J Geotech Geoenviron Eng 135(4):555–565

13. Haines WB (1930) Studies in the physical properties of soil: V. The hysteresis effect in capillary properties, and the modes of moisture associated therewith. J Agric Sci 20:97–116

14. Han Z, Vanapalli SK (2015) Model for predicting the resilient modulus of unsaturated subgrade soil using the soil-water characteristic curve. Can Geotech J 52(10):1605–1619

15. Jin MS, Lee KW, Kovacs WD (1994) Seasonal variation of resilient modulus of subgrade soils. J Transportation Eng 120(4):603–616

16. Khoury NN, Zaman MM (2004) Correlation between resilient modulus, moisture variation, and soil suction for subgrade soils. Transpn Res Rec 1874(1):99–107

17. Konrad JM, Lebeau M (2015) Capillary-based effective stress formulation for predicting shear strength of unsaturated soils. Can Geotech J 52:2067–2076

18. Kumar A, Azizi A, Toll DG (2022) Application of suction monitoring for cyclic triaxial testing of compacted soils. J Geotech Geoenviron Eng 148(4):04022009

19. Kumar A, Azizi A, Toll DG (2022). The influence of cyclic loading frequency on the response of an unsaturated railway formation soil. In Proceedings, Geo-Congress 2022. Charlotte: Geo-Congress

20. Lekarp F, Isacsson U, Dawson A (2000) State of the art. I: resilient response of unbound aggregates. J Transp Eng 126(1):66–75

21. Liang RY, Rabab'ah S, Khasawneh M (2008) Predicting moisture-dependent resilient modulus of cohesive soils using soil suction concept. J Transpn Engng 134(1):34–40

22. Lourenço SDN, Gallipoli D, Toll D, Augarde C, Evans F, Medero G (2008) Calibrations of a high suction tensiometer. Géotechnique 58(8):659–668

23. Mamou A, Priest JA, Clayton CRI, Powrie W (2018) Behaviour of saturated railway track foundation materials during undrained cyclic loading. Can Geotech J 55(5):689–697

24. McCartney JS, Khosravi A (2013) Field monitoring system for suction and temperature profiles under pavements. J Perform Constr Facil 27(6):818–825

25. Miller CJ, Yesiller N, Yaldo K, Merayyan S (2002) Impact of soil type and compaction conditions on soil water characteristic. J Geotech Geoenviron Eng 128:733–742

26. Musso G, Azizi A, Jommi C (2020) A microstructure-based elastoplastic model to describe the behaviour of a compacted clayey silt in isotropic and triaxial compression. Can Geotech J - 57(7):1025–1043

27. Ng CWW, Zhou C, Yuan Q, Xu J (2013) Resilient modulus of unsaturated subgrade soil: experimental and theoretical investigations. Can Geotech J 50(2):223–232

28. Oh JH, Fernando EG, Holzschuher C, Horhota D (2012) Comparison of resilient modulus values for Florida flexible mechanistic empirical pavement design. Int J Pavement Eng 13(5):472–484

29. Oloo SY, Fredlund DG (1998) The application of unsaturated soil mechanics theory to the design of pavements. In: Proceedings 5th international conference on the bearing capacity of roads and airfields, Tapir Academic Press, Trondheim p 1419–1428

30. Pham HQ, Fredlund DG, Barbour SL (2005) A study of hysteresis models for soil-water characteristic curves. Can Geotech J 42(6):1548–1568

31. Qian J, Lin Z, Shi Z (2022) Soil-water retention curve model for fine-grained soils accounting for void ratio-dependent capillarity. Can Geotech J 59(4):498–509

32. Romero E, Della Vecchia G, Jommi C (2011) An insight into the water retention properties of compacted clayey soils. Géotechnique 61(4):313–328

33. Seed HB, Chan CK, Lee C E (1962) Resilience characteristics of subgrade soils and their relation to fatigue failures. In: Proceedings of the international conference on structural design of asphalt pavements, Ann Arbor, Michigan, p 611–636

34. Sivakumar V, Kodikara J, O'Hagan R, Hughes D, Cairns P, McKinley JD (2013) Effects of confining pressure and water content on performance of unsaturated compacted clay under repeated loading. Géotechnique 63(8):628–640

35. Stirling RA, Toll DG, Glendinning S, Helm PR, Yildiz A, Hughes PN, Asquith JD (2020) Weather–driven deterioration processes affecting the performance of embankment slopes. Géotechnique 71(11):957–969

36. Tarantino A (2009) A water retention model for deformable soils. Géotechnique 59(9):751–762

37. Tarantino A, Tombalato S (2005) Coupling hydraulic and mechanical behavior in unsaturated compacted clay. Géotechnique 55(4):307–317

38. Toll DG, Lourenço SDN, Mendes J (2013) Advances in suction measurements using high suction tensiometers. Eng Geol 165(24):29–37

39. Tuller M, Dani O, Dudley LM (1999) Adsorption and capillary condensation in porous media: liquid retention and interfacial configurations in angular pores. Water Resour Res 35(7):1949–1964

40. Vanapalli SK, Fredlund DG, Pufahl DE (1999) The influence of soil structure and stress history on the soil–water characteristics of a compacted till. Géotechnique 49(2):143–159

41. Van Genuchten MT (1980) A closed-form equation for predicting the hydraulic conductivity of unsaturated soils. Soil Sci Soc Am J 44(5):892–898

42. Wheeler SJ, Sharma RS, Buisson MSR (2003) Coupling of hydraulic hysteresis and stress–strain behaviour in unsaturated soils. Géotechnique 53(1):41–54

43. Yang SR, Lin HD, Kung HS, Huang WH (2008) Suction-controlled laboratory test on resilient modulus of unsaturated

compacted subgrade soils. J Geotech Geoenviron Eng 134(9):1375–1384

44. Zhai Q, Rahardjo H, Satyanaga A, Dai G, Zhuang Y (2020) Framework to estimate the soil-water characteristic curve for soils with different void ratios. Bull Eng Geol Environ 79:4399–4409

45. Zhou A, Huang R, Sheng D (2016) Capillary water retention curve and shear strength of unsaturated soils. Can Geotech J 53:974–987

46. Zhou C, Ng CWW (2016) Simulating the cyclic behaviour of unsaturated soil at various temperatures using a bounding surface model. Géotechnique 66(4):344–350